

Damping of Large-Amplitude Plasma Waves Propagating Perpendicular to the Magnetic Field

J. M. Dawson, V. K. Decyk, Robert W. Huff, I. Jechart, T. Katsouleas, J. N. Leboeuf,
B. Lembege, R. M. Martinez, Y. Ohsawa, and S. T. Ratliff

Department of Physics, University of California, Los Angeles, California 90024

(Received 20 September 1982)

Computer simulations of magnetosonic waves, velocity-shell instabilities, and upper-hybrid heating show evidence of a general damping mechanism for large-amplitude electrostatic waves propagating perpendicular to a magnetic field: Particles trapped by a wave of frequency ω and phase velocity V_{ph} see an electric field $V_{ph} \times B$, which accelerates them parallel to the wave front until the $v \times B$ force is large enough for detrapping. For $\omega \gg \omega_c$, velocities as large as $(\omega/4\omega_c)V_{ph}$ can be attained, within a time $\omega_c t \approx \omega/4\omega_c$.

PACS numbers: 52.35.Mw, 52.35.Fp, 52.65.+z

Plasma waves propagating perpendicular to a magnetic field are not as easily damped or absorbed as their parallel propagating counterparts. In a thermal plasma, simulations (Kamimura, Wagner, and Dawson¹) have confirmed that in the limit as the magnetic field approaches zero, the Bernstein modes, which themselves are undamped, collectively act as a single quasi-mode which damps according to the usual Landau damping rate for electrostatic waves in the absence of an applied magnetic field. This Landau-like damping arises from the phase mixing of an infinite set of closely spaced frequencies, which are nearly all harmonics of the cyclotron frequency.

For nonzero cyclotron frequency much smaller than the wave frequency, waves can be stochastically damped if their phase velocity is comparable to, or less than, the particle thermal velocity (Sagdeev and Shapiro,² and Karney³). Then a significant number of particles can move in nearly constant phase with the wave at some points in their Larmor orbits. In effect, the particles receive random impulses at these resonant points, with corresponding changes in the wave energy.

The minimum wave amplitude necessary for stochastic damping increases as the phase velocity increases beyond the thermal velocity, and approaches the cold-trapping threshold in the limit. For such large amplitudes, the electric force of the wave initially greatly exceeds the $v \times B$ force, whereas Karney assumed the wave to be a small perturbation on the Larmor motion. Particles can now be temporarily trapped and accelerated parallel to the wave front (Forslund, Morse, and Nielson⁴; Sagdeev and Shapiro²; and Sugihara and Midzuno⁵). They become detrapped as the $v \times B$ force overcomes the electrostatic force of the wave. This can result either from

an increase in v , or from a decrease in the electric field, e.g., via damping of the wave, or via motion of the particles to a region of lower wave amplitude. By this mechanism the wave can rapidly lose most of its energy in producing a few fast particles.

We examine this mechanism in some detail before discussing relevant simulation results. Under the combined influence of an electrostatic wave, $-E \sin(ky - \omega t)$, propagating in the positive y direction with phase velocity $V_{ph} = \omega/k$, and a z -direction magnetic field with cyclotron frequency ω_c , the particle equations of motion in the wave frame are

$$\ddot{x} = \omega_c (V_{ph} + \dot{y}), \quad (1)$$

$$\ddot{y} = -\omega_c \dot{x} - (qE/m) \sin ky. \quad (2)$$

Integration of Eq. (1) yields

$$\dot{x} = \dot{x}_0 + \omega_c (V_{ph} t + y - y_0), \quad (3)$$

where the subscripts 0 denote initial values. Insertion of Eq. (1) into the derivative of Eq. (2) gives

$$\ddot{y} = -\omega_B^2 \dot{y} - \omega_c^2 V_{ph}, \quad (4)$$

where

$$\omega_B^2(y) = \omega_c^2 + (qEk/m) \cos ky. \quad (5)$$

Equation (4) describes sinusoidal oscillations of \dot{y} about an average velocity

$$V_{av}(y) = -(\omega_c/\omega_B)^2 V_{ph} \quad (6)$$

with frequency ω_B , provided the oscillation amplitude is small. Equation (6) shows that the oscillating particle falls behind the wave, at a rate increasing to V_{ph} (i.e., zero velocity in the laboratory frame) as $\cos ky \rightarrow 0$, at which time detrapping occurs. For this small-oscillation case, we may use the approximation $\ddot{y} \approx 0$ in

Eq. (2) to obtain $\dot{x} = -(qE/m\omega_c) \text{sink}y$, which approaches an escape value

$$V_{\text{esc}} = (qE/m\omega_c) \text{sgn}(q) \equiv V_E \text{sgn}(q) \quad (7)$$

as detrapping occurs. Note that this value is the $E \times B$ drift velocity, and (except for sign) is independent of particle charge, mass, and initial conditions, although, by Eq. (3), these parameters do affect the time of detrapping. This result differs from that of Ref. 5, where a small-oscillation final velocity, $\dot{x} = \pi V_E + \dot{x}_0$, is obtained.

For large oscillations, the precise \dot{x} attained at detrapping is a function of the initial conditions. However, Eq. (2) shows that if $\dot{x} \text{sgn}(q) > V_E$, the y acceleration is everywhere negative, and trapping is not possible. If $\dot{x} \text{sgn}(q) < V_E$, there is a region of positive acceleration, but this may not be sufficient to reflect a large-oscillation particle. Thus, Eq. (7) should be considered as an upper limit on $|\dot{x}|$ in the general case. Conceivably, depending upon the phase of the oscillation when this limit is reached, $|\dot{x}|$ might exceed V_E by as much as $2\pi V_{\text{ph}}$ [cf. Eqs. (3) and (5)] if the particle must complete the oscillation before falling behind the wave. But this could happen only for small oscillations, for which $\dot{y} \approx V_{\text{av}} \approx -V_{\text{ph}}$ and hence $\ddot{x} \approx 0$, so that \dot{x} is insensitive to the exact time of escape as \dot{x} approaches V_{esc} .

We are interested in this mechanism for $\omega \gg \omega_c$ and V_{ph} large relative to the thermal velocity. Then the cold trapping condition, $2(qE/mk)^{1/2} \gtrsim V_{\text{ph}}$, must be satisfied, and gives the threshold condition,

$$V_E \gtrsim (\omega/4\omega_c) V_{\text{ph}}, \quad (8)$$

where we hereafter ignore the sign of the charge. After detrapping, a particle will still interact stochastically with the wave if its velocity is below the Karney maximum stochastic velocity,

$$V_{\text{MS}} \approx (32\omega/\pi\omega_c)^{1/3} V_E^{2/3} V_{\text{ph}}^{1/3}. \quad (9)$$

Note that $V_{\text{MS}} > V_E$ unless V_E greatly exceeds the threshold value of Eq. (8), which in general will not occur because the wave becomes heavily damped when the threshold given by Eq. (8) is reached. However, the mechanism described here is not really stochastic since the particle is accelerated to V_E in one short impulse. Since $V_E \approx V_{\text{MS}}$, this suggests that in many cases this systematic acceleration may dominate over stochastic heating.

Plasma instabilities which grow from a low noise level will not be affected by this mecha-

nism until roughly the trapping threshold amplitude of Eq. (8) is attained. Rapid energy absorption by trapped particles is then expected to saturate the growing wave at this level. This saturation should be accompanied by the production of fast particles, up to a limit of $(\omega/4\omega_c)V_{\text{ph}}$, which can greatly exceed the phase velocity of the wave itself. Since this value of \dot{x} generally dominates the \dot{x}_0 and $y - y_0$ terms of Eq. (3), the wave saturation and particle production should occur within a time

$$\omega_c t \approx \omega/4\omega_c. \quad (10)$$

This mechanism is illustrated in Fig. 1, which shows a representative particle orbit in laboratory-frame velocity space. The equations of motion were integrated for many particles initially at rest in the laboratory frame, but with different initial positions. A given electric field wave was used, with parameters $V_E = 10$, $V_{\text{ph}} = 0.764$, and $\omega = 3\omega_c$; thus V_E exceeds the 0.57 threshold value of Eq. (8). The predicted initial frequency of oscillation in the y direction is $\omega_B(0) = 6.35\omega_c$, which gives an initial average velocity in the laboratory frame of $V_{\text{av}}(0) + V_{\text{ph}} = 0.745$, indistinguishable from V_{ph} itself. These oscillations are prominent in the figure, and this signature could

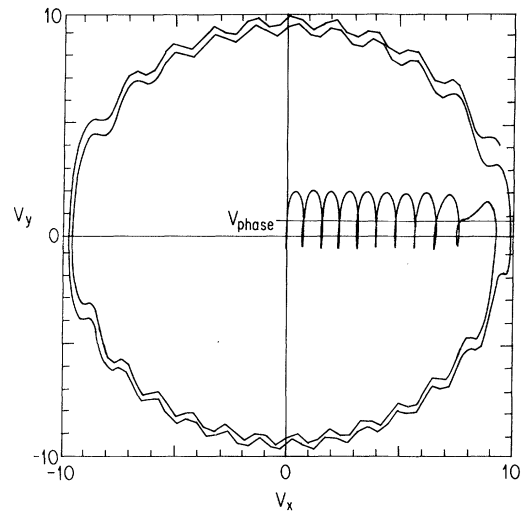


FIG. 1. Velocity-space orbit of a particle of positive charge moving in a strong electrostatic wave propagating in the positive y direction, with a uniform magnetic field directed out of the page. The particle is initially trapped, and oscillates in v_y while accelerating in the x direction. Upon escape, it is left on a modulated Larmor orbit with velocity much larger than the phase velocity, $V_{\text{ph}} = 0.764$, and slightly smaller than the $E \times B$ drift velocity $V_E = 10$.

serve to identify the mechanism in more realistic simulations. The observed decrease in amplitude with decreasing frequency (i.e., increasing intervals in \dot{x}) is a consequence of adiabatic invariance,⁶ whereby the mean square value of \dot{y} over a full cycle is inversely proportional to the period. Adiabatic invariance breaks down as detrapping is approached, where the equality of frequencies, $\omega_B \approx \omega_c$ [cf. Eq. (5)] causes degeneracy of the two-dimensional system, and the explicit time dependence of the reduced one-dimensional system is no longer slow relative to the bounce frequency ω_B . The measured $\dot{x} = 9$ at detrapping is less than the limiting value, $V_E = 10$, because the large oscillations permit early detrapping, at time $\omega_c t = 12$. The particle gains much energy while trapped and is left on a large Larmor orbit, within only two cyclotron periods. This Larmor orbit is slightly perturbed by the wave, which, since $V_{MS} = 13.3$, is expected to produce further stochastic energy changes, either gains or losses, over much longer times.

These same parameters were used for a numerical study of the discrepancy between Eq. (7) and the result of Ref. 5. For a wide range of initial positions and velocities, including \dot{x}_0 as large as 9, the maximum attainable \dot{x} was found to be well approximated by $V_E + V_{ph}$. Repetition with $V_{ph} = 4$ gave the same result. In both cases, the value V_E could be exceeded only with particles initially almost at rest in the wave frame, and this value was then exceeded by an amount small relative to the previously conjectured $2\pi V_{ph}$. The \dot{x} limit was found to be essentially independent of \dot{x}_0 . Thus, the results are in definite disagreement with the limit expression, $\pi V_E + \dot{x}_0$, of Ref. 5, in regard to both the value of the V_E coefficient and the presence of the \dot{x}_0 term.

The clearest evidence for this mechanism in self-consistent simulations has been seen in a study of ion acceleration by large-amplitude magnetosonic waves.⁷ Figure 2 presents the ion velocity-space distributions at times $\omega_{ci} t = 3, 6, 9,$ and 12 . The trapped ions first appear in Fig. 2(b), where they form an arc concave to the left in the upper right-hand portion of the plot. After detrapping, the ions are left in a large Larmor orbit, clearly separated from the bulk of the ion distribution in Figs. 2(c) and 2(d). The magnetosonic wave is traveling to the right, and reaches peak amplitude at the time of Fig. 2(b). The corresponding peak value of $V_E = 1.5$ slightly exceeds the cold-trapping threshold value, $(\omega/4\omega_{ci})V_{ph} = 1.2$, from Eq. (8). The wave amplitude decreases

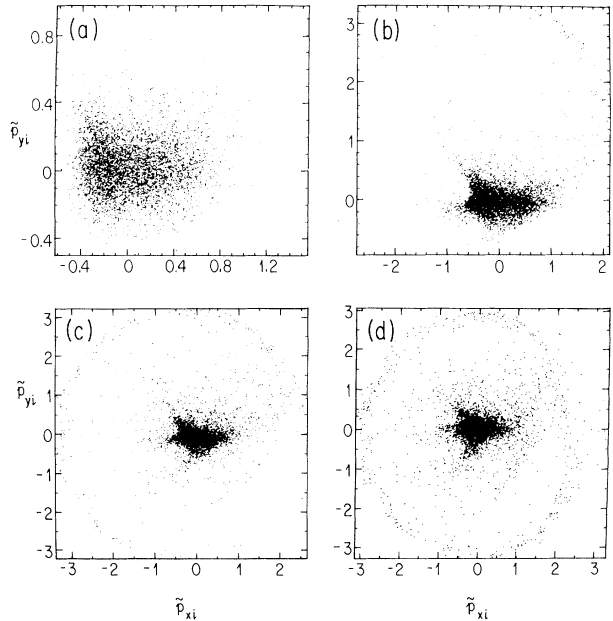


FIG. 2. (a)–(d) Ion momentum-space distributions at times $\omega_{ci} t = 3, 6, 9,$ and 12 , respectively, in the presence of a magnetosonic wave propagating in the x direction. The normalized-momentum scales are essentially velocity scales, since $c = 10$ in the same units. Note the differing numerical scales on the four plots.

es to $V_E = 1.0$ after the peak as the heating of the bulk ions lowers the trapping threshold. Ion phase-space plots of V_x vs x [cf. Fig. 1(c) of Ref. 7] show the characteristic trapped-particle structure at the time of the wave peak and beyond. The large Larmor orbit of Fig. 2 shows an escape velocity, $V_{esc} = 3.0$, which exceeds V_E but agrees well with the expression, $V_E + V_{ph} = 2.9$, reported above for the maximum escape velocity attained in the single-particle study. Equations (3) and (5) predict that the trapped-ion velocity parallel to the wave front should reach the values $V_E = 1.5$ and $V_{esc} = 3.0$ in times $\omega_B(0) t \approx 2.4$ and 4.7 , respectively. Thus, no more than one bounce should occur before detrapping, as seen in Fig. 2.

A second category of simulations that shows evidence of wave damping via this trapping mechanism is a study of spherical velocity-shell instabilities using a $2\frac{1}{2}$ -dimension electrostatic particle code with a fixed magnetic field perpendicular to the electric grid plane. For cases with the strongest instability, the electrostatic field reaches 25% to 110% of the cold-trapping threshold given by Eq. (8), and is then damped within a time $\omega_c t \approx 3-5$, or several times the single-particle estimate of Eq. (10) with $\omega \approx 3\omega_c$.

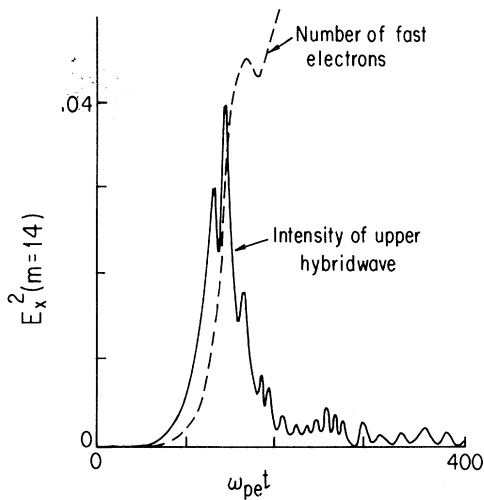


FIG. 3. Growth and decay of the forward-scattered electrostatic upper-hybrid wave (mode 14) associated with Raman backscattering. The wave peak coincides with a sudden increase in the number of fast electrons, here defined as having a perpendicular velocity component exceeding the phase velocity of the upper-hybrid wave, which in turn remains 3 to 4 times the bulk electron thermal velocity throughout the simulation. At the peak of the electrostatic wave amplitude about 6% of the electrons have been accelerated to high energy.

This damping is accompanied by the production of a few fast particles (approximately 0.2% out of the 384 000 cold Maxwellian background particles) with velocities up to twice the phase velocity and clearly separated (by 10 or more times the thermal speed) from the main Maxwellian. The energy of these fast particles is comparable

to that lost by the waves during damping.

Evidence of this damping mechanism also appears in simulations of the Raman backscattering of extraordinary waves in a collisionless uniform magnetized plasma using a $1\frac{1}{2}$ -dimension electromagnetic particle code with k perpendicular to B_0 . The pump wave causes sufficient heating to lower the trapping threshold below the value given by Eq. (8), and the peak amplitude of the forward-scattered electrostatic upper-hybrid wave agrees with this lower warm-trapping threshold.⁸ The damping of this wave is simultaneous with the generation of a small number of fast electrons with velocities up to 7 times the thermal velocity, as shown in Fig. 3.

This work was partially supported by the National Science Foundation and the U. S. Department of Energy.

¹T. Kamimura, T. Wagner, and J. M. Dawson, *Phys. Fluids* **21**, 1151 (1978).

²R. Z. Sagdeev and V. D. Shapiro, *Pis'ma Zh. Eksp. Teor. Fiz.* **17**, 389 (1973) [*JETP Lett.* **17**, 279 (1973)].

³C. F. F. Karney, *Phys. Fluids* **21**, 1584 (1978).

⁴D. W. Forslund, R. L. Morse, and C. W. Nielson, *Phys. Rev. Lett.* **27**, 1424 (1971).

⁵R. Sugihara and Y. Midzuno, *J. Phys. Soc. Jpn.* **47**, 1290 (1979).

⁶Herbert Goldstein, *Classical Mechanics* (Addison-Wesley, Reading, Mass., 1950), p. 316.

⁷B. Lembege, S. T. Ratliff, J. M. Dawson, and Y. Ohsawa, UCLA Plasma Physics Group Report No. PPG-683 (to be published).

⁸T. P. Coffey, *Phys. Fluids* **14**, 1402 (1971).